Photocatalytic Degradation of Methyl Orange in Simulated Textile Wastewater Using Iron Terephthalate Metal–Organic Framework under Visible Light Irradiation

Eden S. Erasga[1,*], Chloe Justin Bigornia[2], Yna Isabel Dimaano[2], and Quinn Lendyll Teope[2]

[1]College of Arts and Science, Mapua Malayan Colleges Laguna, Cabuyao City, Philippines
[2]Department of Chemical Engineering, Mapua Malayan Colleges Laguna, Cabuyao City, Philippines
Email: eserasga@mcl.edu.ph (E.S.E.); cabigornia@live.mcl.edu.ph (C.J.B.); yindimaano@live.mcl.edu.ph (Y.I.D.); qlteope@live.mcl.edu.ph (Q.L.T.)
*Corresponding author

Manuscript received May 4, 2025; revised July 28, 2025; accepted September 25, 2025; published July 22, 2026

Abstract*—The discharge of persistent organic dyes from industrial wastewater into aquatic environments poses a significant environmental threat, creating an urgent need for advanced and sustainable treatment technologies. Among emerging solutions, iron-based Metal-Organic Frameworks (MOFs) have shown great promise as efficient photocatalysts. However, the synergistic effects of Materials Institute Lavoisier (MIL)-53(Fe) combined with hydrogen peroxide (H_2O_2) under visible light irradiation for dye degradation remain poorly understood. To address this gap, this study systematically investigates the photocatalytic degradation of Methyl Orange (MO) using a MIL-53(Fe) photocatalyst activated with H_2O_2 under visible light. The MIL-53(Fe) material was synthesized and characterized using Fourier-Transform Infrared Spectroscopy (FTIR) and Scanning Electron Microscopy (SEM) to confirm its structural and morphological properties. The photocatalytic performance was assessed by optimizing key parameters, including the initial pH and H_2O_2 dosage. Kinetic analyses and comparative experiments were conducted to elucidate the degradation mechanism. Results demonstrated a remarkable 98.75% degradation of MO within 60 min, following pseudo-first-order kinetics. This performance significantly outperformed visible light irradiation alone, which achieved only 10.71% degradation. Mechanistic studies further revealed that hydroxyl radicals (•OH) and photo-generated holes (h+) are the primary reactive species driving the degradation process. These findings highlight the high efficiency and tunability of MIL-53(Fe) as an environmentally benign photocatalyst. The study highlights its potential application in advanced wastewater treatment technologies under solar-simulated conditions, providing a scalable and sustainable approach for dye mineralization in industrial effluents.

***Keywords*—photocatalytic degradation, metal–organic frameworks, Materials Institute Lavoisier (MIL)-53(Fe), methyl orange, hydrogen peroxide, visible light irradiation**

I. Introduction

The textile industry is a significant contributor to global water pollution, discharging approximately 280,000 tons of synthetic dyes into surface waters annually [1]. In the Philippines, the continued expansion of this sector has led to increasing volumes of dye-containing effluents, prompting regulatory interventions, such as the Department of Environment and Natural Resources Administrative Order (DAO) 2021-19, which imposes effluent standards, including color as a key parameter, for discharge into Class C waters.

Azo dyes, particularly Methyl Orange (MO), are among the most persistent organic pollutants due to their complex aromatic structures and resistance to biodegradation. The release of intensely colored wastewater not only degrades the visual quality of water bodies but also disrupts aquatic ecosystems by limiting light penetration and impairing photosynthetic activity [2]. Additionally, these pollutants contribute to increased biochemical and chemical oxygen demand and may contain hazardous compounds with mutagenic or carcinogenic potential, thereby posing risks to both the environment and human health [3]. Conventional wastewater treatment techniques are generally ineffective for dyes like methyl orange due to their high resistance to both biological and chemical degradation [4].

Several conventional methods, such as reverse osmosis and ion exchange, have been employed for dye removal [5–7]. However, high operational costs and complex procedures often limit their widespread use [8]. Adsorption provides rapid dye removal, operational simplicity, and low cost [9], but merely transfers pollutants onto solids, creating secondary waste that must be disposed of or regenerated [10]. Coagulation–flocculation is effective for treating low dye concentrations in textile wastewater [11], as it aggregates dye particles for removal. Nevertheless, this process produces large amounts of sludge, introduces chemical residues, and its performance varies with dye chemistry and operational conditions [12]. Biological treatments are environmentally benign but often slow and unable to degrade resistant dyes fully. This results in incomplete breakdown and potentially toxic intermediates, which are particularly problematic given the low biodegradability of many industrial effluents [13]. These limitations underscore the need for more effective methods that can comprehensively remove and ideally completely mineralize dye contaminants.

Advanced Oxidation Processes (AOPs) rely on the generation of highly reactive hydroxyl radicals (·OH) to non-selectively degrade persistent organic pollutants, including synthetic dyes [14]. Techniques such as photocatalysis and photo-Fenton reactions have demonstrated considerable effectiveness in mineralizing complex dye molecules that are resistant to conventional methods, including adsorption, coagulation–flocculation, and biological treatment [15]. Unlike these traditional approaches, which often result in secondary waste, incomplete degradation, or require extensive post-treatment, AOPs offer the advantage of complete mineralization, converting organic dyes into carbon dioxide and water [16], which makes them particularly suitable for treating

recalcitrant, non-biodegradable dyes commonly found in textile and industrial effluents. However, large-scale application of AOPs is often constrained by factors such as high energy consumption, prolonged reaction times, the use of expensive or hazardous reagents, and limited efficiency under ambient light conditions [17]. To overcome these challenges, visible-light-driven systems—particularly those harnessing solar energy—have gained increasing attention for their potential to improve both the sustainability and practicality of AOPs. Nevertheless, conventional photocatalysts are still hindered by issues such as rapid electron-hole recombination and limited photoactivity in the visible spectrum, which reduce their overall efficiency and applicability [18].

To overcome the limitations associated with conventional photocatalysts in AOPs, considerable research has focused on developing advanced materials with enhanced light absorption, charge separation, and structural stability. Among these new materials, Metal-Organic Frameworks (MOFs) have shown remarkable promise. MOFs are crystalline porous materials constructed from metal ions or clusters coordinated to organic linkers, resulting in highly ordered structures with exceptional surface area, tunable porosity, and semiconducting properties [19]. These attributes make MOFs particularly attractive for photocatalytic applications. Specifically, MOFs can enhance the generation of Reactive Oxygen Species (ROS) under light irradiation in AOPs [20]. Among MOF-based photocatalysts, MIL-53(Fe)—an iron-based member of the Materials Institute Lavoisier (MIL) family—has garnered significant attention. MIL-53(Fe) is noted for its strong visible-light activity and ability to catalyze the degradation of recalcitrant dyes through ROS production. It offers several advantages over conventional semiconductors, including high structural stability, low toxicity, and excellent photocatalytic performance across a range of environmental conditions [21]. Its cost-effectiveness and responsiveness to visible light further support its potential as a sustainable photocatalyst for the degradation of industrial dyes.

This study presents the first comprehensive evaluation of MIL-53(Fe) as a visible-light-activated photocatalyst for the degradation of MO in the presence of H_2O_2, addressing a critical gap in current photocatalytic dye treatment research. While MIL-53(Fe) has been recognized for its photocatalytic potential, its synergistic performance with H_2O_2 under visible light has not been systematically investigated. In this work, the catalyst was synthesized and characterized using Fourier-Transform Infrared Spectroscopy (FTIR) and Scanning Electron Microscopy (SEM), and its photocatalytic efficiency was assessed under varying pH conditions, H_2O_2 concentrations, and reaction durations. The results provide new insights into the mechanisms and operational parameters that influence MO degradation, demonstrating the relevance of MIL-53(Fe) for solar-assisted, environmentally sustainable wastewater treatment applications.

II. Literature Review

Photocatalysis, a key Advanced Oxidation Process (AOP), has seen remarkable progress since Fujishima and Honda's discovery of photochemical water splitting in 1972 [22]. This technique employs light-activated catalysts, including TiO_2 and various metal oxides and sulfides such as ZnO, WO_3, CdS, and ZnS, to degrade complex and recalcitrant pollutants in water and air, offering an effective solution for environmental remediation [23]. Despite their effectiveness, traditional inorganic photocatalysts face challenges including difficult recovery, agglomeration, and low solar-to-chemical conversion efficiency, which hinder large-scale application [21]. These limitations have driven increasing interest in the development of novel photocatalysts with enhanced activity and stability for practical environmental applications.

MIL-53(Fe), a Metal-Organic Framework (MOF), has recently gained prominence as a heterogeneous photocatalyst for the degradation of water pollutants under visible or solar irradiation. MOFs are crystalline, porous materials composed of metal clusters, serving as inorganic nodes, coordinated to organic linkers, forming robust three-dimensional networks [21]. While various transition metals can be used to synthesize MOFs, non-noble metals such as iron, cobalt, copper, zinc, titanium, and zirconium are preferred due to their abundance and cost-effectiveness and have demonstrated potential in water treatment, hydrogen production, CO_2 capture, and gas storage [24]. Among them, MIL-53(Fe) is a notable iron-based MOF consisting of infinite one-dimensional chains of –Fe–O–O–Fe–O–Fe– units, cross-linked by bis-bidentate terephthalate (1,4-benzenedicarboxylate) ligands [23]. This structure forms diamond-shaped channels running parallel to the inorganic chains, as illustrated in Fig. 1 and described by Munn *et al.* [25].

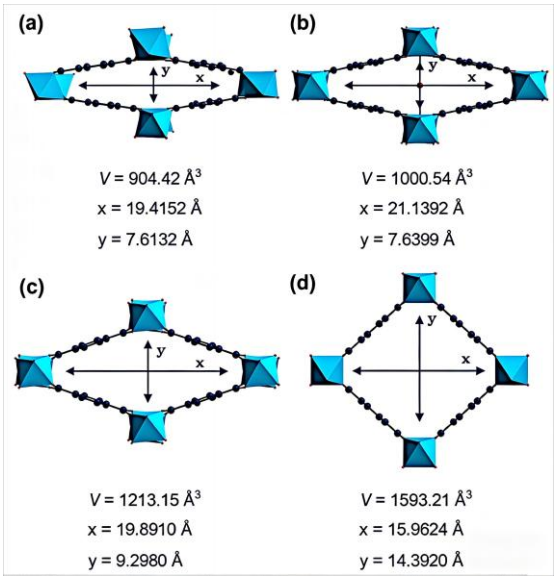

Fig. 1. Structural representations of MIL-53(Fe): (a) dehydrated form, (b) hydrated form showing water molecules (oxygen shown as red spheres), (c) half-open MIL-53(Fe)[2,6-lutidine], and (d) fully open MIL-53(Fe)[2,6-lutidine, H_2O]. Guest molecules are omitted for clarity except in (b). Adapted from [25].

This 3D structure imparts high surface area, structural stability, and semiconducting properties. The empty d orbitals of Fe can interact with the Lowest Unoccupied Molecular Orbitals (LUMOs) of the organic linkers to form the conduction band [23]. In addition, the organic bridging ligands function as light-harvesting antennas, enabling Ligand-to-Cluster Charge Transfer (LCCT) under

irradiation [19]. Upon light exposure, electron excitation and subsequent charge transfer occur within the MOF structure, positioning MIL-53(Fe) as a promising heterogeneous photocatalyst for environmental applications [23].

In a recent study [26], MIL-53(Fe) synthesized via a solvothermal method exhibited limited photocatalytic activity under simulated solar light, removing less than 10% of phenol after 3 h. However, the addition of oxidants such as ozone, persulfate, or hydrogen peroxide significantly enhanced its performance, achieving complete pollutant degradation within 2 h. These findings underscore the synergistic effect of MIL-53(Fe) and oxidizing agents in advanced photocatalytic processes.

A notable study by Dinh *et al*. [27] explored the enhancement of photocatalytic performance through the addition of Hydrogen Peroxide (H_2O_2), which facilitates the *in-situ* generation of highly reactive hydroxyl radicals (•OH). These radicals possess strong oxidative potential and can non-selectively mineralize a wide range of organic pollutants into CO_2, H_2O, and inorganic ions. The experimental results demonstrated that the combination of UV irradiation, 10 mM H_2O_2, and 0.05 g of MIL-53 led to the complete degradation of Methylene Blue (MB) within 60 min, highlighting the synergistic effect of the catalyst and oxidant in achieving rapid and efficient pollutant removal.

Further investigations have explored the application of MIL-53(Fe), an iron terephthalate-based metal-organic framework synthesized via a facile solvothermal method, as a heterogeneous photocatalyst capable of activating H_2O_2 under visible light irradiation. Under visible light irradiation, the electrons in the Fe(III) centers on the MIL-53(Fe) become excited and jump from the valence band to the conduction band to form electrons (e^-) and holes (h^+) that lead to the generation of ROS (reactive oxygen species).

$$H_2O_2 + e^- \rightarrow HO_2\bullet + OH^-$$
$$H_2O_2 + h^+ \rightarrow OH\bullet + OH^-$$

H_2O_2, as an efficient scavenger, could capture the photoinduced electrons in the excited MIL-53(Fe) to form more •OH radicals.

$$\text{MIL-53(Fe)} + h\nu \rightarrow h+ + e^-$$
$$H_2O_2 + e^- (\text{MIL-53(Fe)}) \rightarrow OH\bullet + OH^-$$

Ai *et al.* [28] reported that complete degradation of 10 mg/L Rhodamine B (RhB) was achieved within 50 min using 0.4 g/L MIL-53(Fe) and 20 mM H_2O_2 under illumination from a 500 W tungsten lamp. The catalytic system exhibited a first-order rate constant of 7.94×10^{-2} min^{-1}, significantly higher than the sum of the rate constants from MIL-53(Fe)/visible light and MIL-53(Fe)/H_2O_2 systems (3.57×10^{-2} min^{-1}), indicating a synergistic interaction among the photocatalyst, oxidant, and light source. This cooperative effect markedly enhances photocatalytic efficiency, positioning MIL-53(Fe) as a promising material for the degradation of recalcitrant organic pollutants in aqueous environments.

III. Materials and Methods

A. Preparation of Metal-Organic Framework MIL-53(Fe)

The synthesis of MIL-53(Fe) was conducted using a modified solvothermal procedure based on the method described by Ai *et al*. [28]. In this approach, 0.2703 g of iron (III) chloride hexahydrate ($FeCl_3 \cdot 6H_2O$) and 0.1661 g of terephthalic acid were gradually dissolved in 5 mL of N,N-Dimethylformamide (DMF) under continuous magnetic stirring for 10 min at room temperature. The resulting solution was transferred into a 20 mL Teflon-lined stainless steel autoclave and heated at 150 °C for 2 h. After the reaction, the mixture was cooled to room temperature. The resulting precipitate was separated by centrifugation at 2000 rpm for 30 min. To remove residual solvents and unreacted components, the solid was suspended in 200 mL of distilled water and left overnight. The final product was dried under vacuum at 60 °C for 24 h to obtain MIL-53(Fe) as a yellow powder.

B. Characterization of Metal-Organic Framework MIL-53(Fe)

The chemical structure of the synthesized MIL-53(Fe) was analyzed using Fourier Transform Infrared Spectroscopy (FTIR) to identify characteristic functional groups indicative of successful MOF formation. Surface morphology, particle distribution, and microstructural features were examined using Scanning Electron Microscopy (SEM), providing a detailed visualization of crystal size and surface texture, which are critical to photocatalytic activity.

C. Preparation of Methyl Orange Solution and Standard Curve

A 1000 mg/L stock solution of Methyl Orange (MO) was prepared by dissolving 1000 mg of dye in 1 L of distilled water and stored in an amber container to prevent photodegradation. Working solutions of desired concentrations were obtained by serial dilution of the stock solution. Specifically, simulated textile wastewater solutions of 600 mg/L and 10 mg/L were prepared for experimental applications. To determine the maximum absorbance wavelength (λ_{max}), the 10 mg/L solution was scanned across a range of wavelengths using a UV-Vis spectrophotometer. The wavelength corresponding to the highest absorbance was selected for subsequent measurements. A standard curve was established by preparing MO solutions of 4, 8, 12, 16, and 20 mg/L. The absorbance of each was measured at λ_{max}, and the absorbance values were plotted against the corresponding concentrations to generate a standard curve for the quantitative analysis of dye degradation.

D. Photocatalytic Degradation Experiments

Photocatalytic degradation of MO in the presence of H_2O_2 over MIL-53(Fe) was conducted following a modified procedure based on [15]. A 25 mL aliquot of a 600 mg/L MO solution was used in each experimental run, placed in a 100 mL beaker, and exposed to visible light irradiation using a 500 W tungsten lamp for 100 min. The solutions were continuously stirred at 200 rpm throughout the irradiation process, which was carried out over a period of 100 min. Following irradiation, the reaction mixtures were filtered using Whatman filter paper, and the resulting supernatants were analyzed for residual dye concentration using UV-Vis spectrophotometry.

To evaluate the effect of initial pH on degradation efficiency, the pH of the solution was adjusted to 3, 5, 7, and 9 using 0.1 M HCl or 0.1 M NaOH, and the pH of the

solutions was measured using a calibrated pH meter. Each experimental setup consists of 25 mL of a 200 ppm MO solution, 0.05 g of MIL-53(Fe), and 10 mL of 20 mM H_2O_2. The pH value yielding the highest decolorization efficiency was designated as the optimal condition for subsequent experiments.

Using the optimal pH identified, the influence of H_2O_2 concentration on MO decolorization was investigated. The experiments were conducted under identical conditions, varying H_2O_2 concentrations at 0, 5, 10, 20, and 40 mM. The concentration that achieved the highest degradation efficiency was selected for subsequent analyses.

In addition, the effect of reaction time was also investigated. The reaction time varied from 20 to 100 min with a 20-min step, using the best initial pH and the optimal H_2O_2 concentration determined previously. Each sample was irradiated under the same conditions described above, and the degradation efficiency was assessed as a function of reaction time.

To elucidate the individual roles of each component within the photocatalytic system, a series of control experiments was conducted under well-defined conditions. These included: (i) visible light irradiation only, (ii) visible light with hydrogen peroxide in the absence of the catalyst, (iii) catalyst with hydrogen peroxide in the absence of light (dark conditions), and (iv) visible light with the catalyst but without hydrogen peroxide. In each case, the degradation of Methyl Orange (MO) was monitored to evaluate the relative contributions of light, catalyst, and oxidant, thereby confirming the synergistic effect and necessity of all components for optimal photocatalytic activity.

E. Statistical Analysis

All photocatalytic degradation experiments were performed in two independent trials, each with two replicates. One-way Analysis of Variance (ANOVA) was used to determine whether differences in MO degradation were statistically significant across various experimental parameters, such as initial pH, H_2O_2 concentration, and contact time. When significant differences were observed ($p < 0.05$), Tukey's Honest Significant Difference (HSD) test was conducted as a post hoc analysis to identify the most effective conditions for MO degradation. This statistical approach was also applied to control experiments to determine whether omitting light, catalyst, or H_2O_2 led to a significant decrease in degradation efficiency compared to the complete photocatalytic system, thereby confirming the essential role of each component.

IV. Result and Discussion

A. Characterization of MIL-53(Fe)

The molecular structure and surface functional groups of the synthesized MIL-53(Fe) were analyzed using Fourier-Transform Infrared (FTIR) spectroscopy, as shown in Fig. 2. The spectrum revealed distinct absorption bands characteristic of iron terephthalate frameworks, confirming the successful formation of the MIL-53(Fe) structure.

A prominent series of peaks between 1700 cm^{-1} and 1400 cm^{-1} corresponds to the vibrational modes of carboxylic acid groups from the terephthalic acid linker [29]. Specifically, the absorption band at 1680 cm^{-1} is attributed to C=O stretching, while the peaks at 1543 cm^{-1} and 1396 cm^{-1} are assigned to the asymmetric and symmetric stretching vibrations of coordinated carboxylate groups, respectively [30]. These features are consistent with spectra reported for MIL-53(Fe) in the literature [21, 26–28], indicating that the linker successfully coordinated with the Fe(III) metal centers.

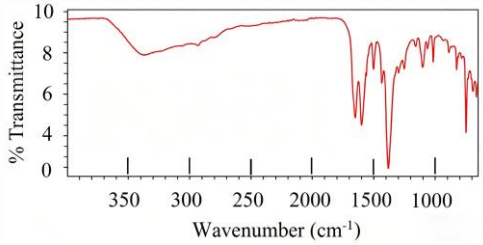

Fig. 2. FTIR spectrum of the synthesized MIL-53(Fe).

Additionally, the absorption at 1594 cm^{-1} supports the presence of metal–ligand interactions, particularly between carboxylate oxygen atoms and iron ions, reinforcing the formation of a stable MOF network [31]. The sharp band at 750 cm^{-1}, associated with out-of-plane C–H bending of the aromatic ring, further confirms the incorporation of the terephthalic acid linker within the framework [32].

A broad band centered at 3440 cm^{-1} is attributed to O–H stretching vibrations from adsorbed water molecules, which are commonly retained within the porous channels of MOFs due to their high surface area and hydrophilicity [33].

These spectral features indicate that the synthesized material exhibits the expected chemical structure of MIL-53(Fe). The FTIR results are in close agreement with recent literature that used similar synthesis conditions and confirmed MIL-53(Fe) formation based on equivalent vibrational assignments [20]. This confirms the effectiveness of the synthesis method and validates the structural integrity of MIL-53(Fe) for photocatalytic degradation applications.

The surface morphology of the synthesized MIL-53(Fe) was examined through Scanning Electron Microscopy (SEM), with representative images shown in Fig. 3, captured at 2500× and 6000× magnification. A heterogeneous morphology is observed, featuring two predominant forms: elongated rod-like crystals (~1–1.5 μm in length) and a more abundant population of pseudo-spherical particles less than 1 μm in diameter. These spherical particles appear to cluster on and around the rods, suggesting a secondary deposition process following primary rod formation—indicative of sequential crystal growth dynamics.

The observed dual-mode morphology of the synthesized MIL-53(Fe), consisting of rod-like and pseudo-spherical particles, is consistent with prior studies that employed solvothermal synthesis methods. Notably, Ai *et al.* [28] reported similar rod-shaped morphologies in MIL-53(Fe) synthesized via a solvothermal route, which reinforces the effectiveness of this method in promoting controlled crystal growth. The observed morphology of the synthesized MIL-53(Fe), featuring both well-defined rod-like particles and smaller, irregular fragments, is consistent with previous studies [34] that employed solvothermal synthesis methods. Furthermore, these findings align with the early structural characterization of MIL-53(Fe) by Loiseau *et al*. [29] and with subsequent morphological analyses that highlight rod-like structures [35]. Taken together, these consistencies validate the successful formation of MIL-53(Fe) using the

solvothermal technique and confirm the material's structural integrity, which is essential for its photocatalytic performance.

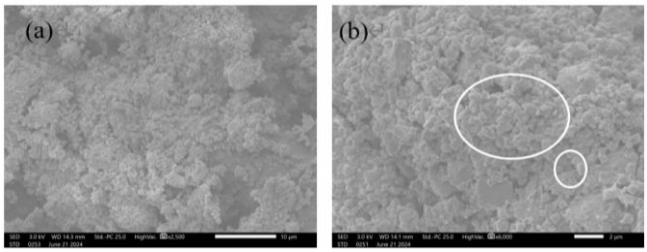

Fig. 3. SEM images of the synthesized MIL-53(Fe) at (a) at 2500× and (b) 6000× magnification.

B. *UV-Vis Spectrophotometry for Methyl Orange: λ_{max} Determination and Calibration*

Accurate quantification of Methyl Orange (MO) was critical for evaluating its photocatalytic degradation efficiency. To determine the optimal detection wavelength, a 10 mg/L MO solution was scanned using UV-Vis spectrophotometry. As depicted in Fig. 4, the resulting absorption spectrum exhibited a distinct peak at 464.98 nm, consistent with the established maximum absorbance range for MO (typically 464–466 nm). This wavelength was subsequently used for all measurements to ensure analytical consistency and precision.

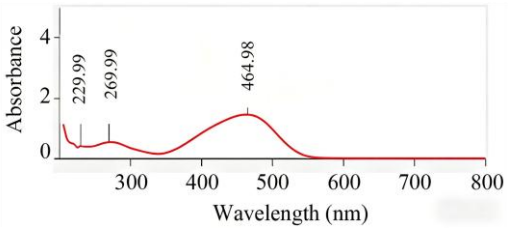

Fig. 4. UV-Vis absorption curve of methyl orange.

To validate the reliability of the method, a standard calibration curve was constructed using MO solutions with concentrations ranging from 4 to 20 mg/L. As shown in Fig. 5, the absorbance exhibited a strong linear relationship with concentration, yielding a correlation coefficient of $R^2 = 0.996$. This excellent linearity confirms the robustness of the spectrophotometric method for accurate and reproducible quantification of MO across all experimental conditions.

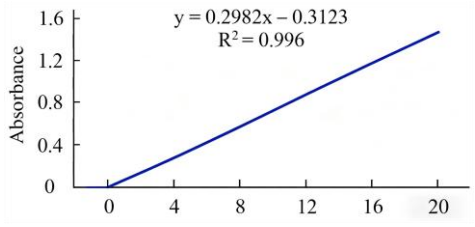

Fig. 5. Standard curve for methyl orange dye.

C. *Photocatalytic Degradation of MO under Visible Light Irradiation*

1) Effect of initial pH on photocatalytic performance of MIL-53(Fe)

Understanding the influence of pH on photocatalytic behavior is vital for optimizing MIL-53(Fe) in practical wastewater treatment applications. The photocatalytic degradation of Methyl Orange (MO) was investigated across a pH range of 3 to 9, revealing consistently high removal efficiencies exceeding 99%, with the peak performance at pH 3 (99.78%) as shown in Fig. 6. This enhanced degradation under acidic conditions aligns with recent studies demonstrating that Fe(III)-based catalysts, such as MIL-53(Fe), exhibit superior Fenton-like activity at low pH due to more efficient activation of H_2O_2, resulting in increased hydroxyl radical (•OH) generation [27]. Furthermore, the catalyst surface becomes positively charged at acidic pH, promoting a stronger electrostatic attraction with the negatively charged MO molecules and enhancing adsorption and degradation efficiency [36].

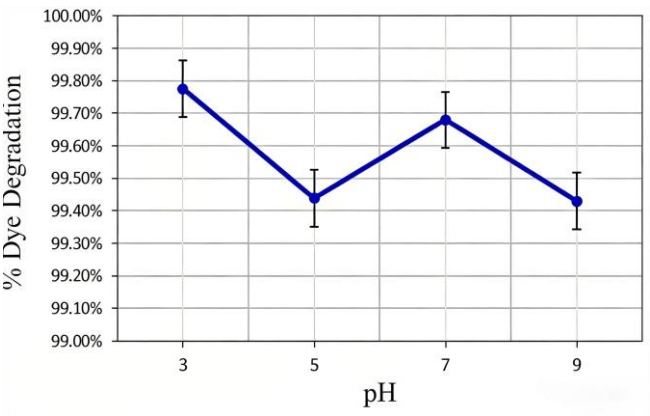

Fig.6. Effect of initial pH on the photocatalytic degradation of methyl orange under visible light irradiation.

Statistical analyses confirmed the significant effect of pH on degradation efficiency (one-way ANOVA, $p < 0.05$), although pairwise comparisons using Tukey's post hoc test indicated no significant differences between individual pH levels, suggesting that MIL-53(Fe) maintains robust catalytic activity across a wide pH spectrum. This broad pH tolerance is a notable advantage for real-world wastewater treatment scenarios where precise pH control may be challenging [31]. Collectively, these findings corroborate and extend current understanding of MIL-53(Fe) photocatalysis, highlighting its practical potential and stability under diverse operational conditions.

2) Effect H_2O_2 Concentration on Photocatalytic Performance of MIL-53(Fe)

Hydrogen peroxide plays a dual role in photocatalytic systems, acting both as a source of reactive oxygen species and, at higher concentrations, as a scavenger of radicals. To determine the optimal H_2O_2 dosage for effective MO degradation, MIL-53(Fe) was tested across a concentration range of 0 to 40 mM. As shown in Fig. 7, the degradation efficiency increased with H_2O_2 concentration, reaching a maximum of 99.61% at 10 mM. Beyond this concentration, a slight decrease in efficiency was observed, dropping to 99.30% at 20 mM and 99.26% at 40 mM, indicating that excessive H_2O_2 has an adverse effect on photocatalytic activity.

This trend aligns with findings in other Advanced Oxidation Processes (AOPs), where increased H_2O_2 initially enhances Hydroxyl Radical (•OH) generation through Fenton-like reactions mediated by Fe(III) centers in

MIL-53(Fe), which effectively degrade organic pollutants such as MO [27, 37]. However, at elevated concentrations, excess H_2O_2 can scavenge •OH or react to form less reactive species like hydroperoxyl radicals (HO_2•), reducing the overall oxidative capacity [26]. Additionally, surplus H_2O_2 may compete with dye molecules for adsorption sites on the catalyst surface, limiting effective interaction and degradation. These results underscore the crucial need to optimize oxidant concentration, confirming that 10 mM H_2O_2 offers the optimal balance between radical production and system efficiency for MIL-53(Fe)-mediated photocatalytic degradation.

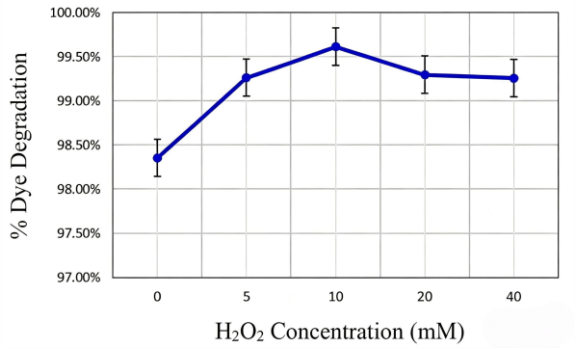

Fig. 7. Effect of H_2O_2 concentration on the photocatalytic degradation of methyl orange under visible light irradiation.

This study's findings are consistent with and expand upon recent reports, underscoring the practical implications of fine-tuning H_2O_2 dosage in visible-light-driven MOF photocatalysts [38].

a) Effect of reaction time on photocatalytic performance of MIL-53(Fe)

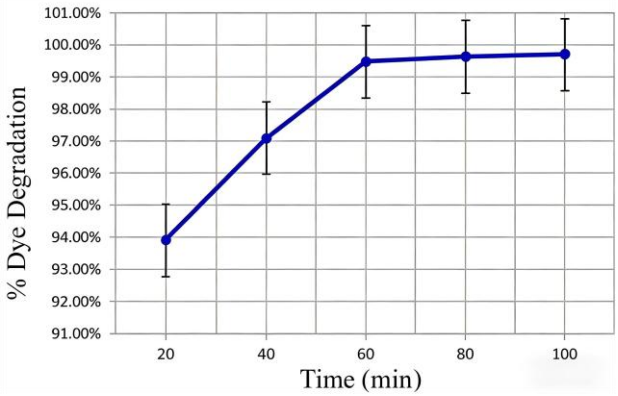

Fig. 8. Effect of reaction time on the photocatalytic degradation of methyl orange under visible light irradiation.

Reaction time is a crucial factor in photocatalytic processes, influencing both degradation efficiency and the overall practicality and energy consumption of treatment systems. This study examined the effect of contact time on MO degradation over intervals ranging from 20 to 100 min. As depicted in Fig. 8, degradation efficiency increased sharply during the initial stages, from 93.91% at 20 min to 99.48% at 60 min, after which the degradation curve plateaued, indicating diminishing returns with extended irradiation. This pattern reflects the dynamic nature of radical-mediated oxidation, where early phases feature vigorous hydroxyl radical generation and abundant MO molecules, facilitating rapid degradation. However, as the reaction progresses and MO concentration decreases, the likelihood of hydroxyl radicals encountering target molecules diminishes, leading to kinetic saturation characteristic of pseudo-first-order reaction kinetics commonly reported in dye photocatalysis [31]. These observations align with previous studies on MIL-53(Fe) [28], which similarly noted a plateau in Rhodamine B degradation under visible light irradiation.

Importantly, extending the reaction time beyond 60 min does not yield significant improvements in degradation efficiency but may unnecessarily increase energy consumption. Therefore, 60 min is identified as the optimal balance between achieving near-complete pollutant removal and maintaining energy-efficient operation. This finding reinforces the importance of optimizing irradiation time for sustainable photocatalytic wastewater treatment applications.

D. Synergistic Roles of Light, Catalyst, and Oxidant in the Photocatalytic Degradation of Methyl Orange

To elucidate the individual contributions of each system component, we conducted a series of control experiments that isolated the effects of visible light, hydrogen peroxide (H_2O_2), and MIL-53(Fe). The outcomes summarized in Table 1 reveal distinct roles for each: visible light alone produced minimal degradation (10.7%), affirming that photocatalysis is insufficient without further participants. When H_2O_2 was added under illumination—without the catalyst—the degradation rate improved modestly to 20.3%, indicating limited radical generation in the absence of MIL-53(Fe). In contrast, the MIL-53(Fe)/H_2O_2 system in dark conditions achieved substantial degradation (70.9%), illustrating a pronounced Fenton-like activity that is independent of light.

Table 1. Control experiments Methyl Orange (MO) degradation under various conditions

Condition	% Dye degradation at 60 min
Visible light only	10.71
H_2O_2 with visible light	20.33
MIL-53(Fe) / H_2O_2 / dark	70.95
MIL-53(Fe) / visible light	98.25
MIL-53(Fe) / H_2O_2 / visible light	98.75

Notably, the complete system, comprising MIL-53(Fe), H_2O_2, and visible light, achieved the highest degradation efficiency (98.8%), indicating a strong synergistic interaction among all components. Light exposure generates electron-hole pairs within MIL-53(Fe), while H_2O_2 enhances the production of hydroxyl radicals (•OH), leading to increased degradation. Our findings are consistent with previously reported mechanisms where MIL-53(Fe) activates H_2O_2 via dual pathways—Fenton-like catalysis and electron capture—to form •OH radicals under visible light [28].

Moreover, the photocatalytic efficiency proved to be highly dependent on the solution pH. Like in other Fe-MOF systems, acidic conditions favored radical formation and dye breakdown, whereas higher pH values led to decreased efficiency due to reduced H_2O_2 stability and radical reactivity [18, 27]. This emphasizes the importance of optimizing operational parameters to maximize ROS production and degradation efficiency.

To better understand the underlying mechanism of

photocatalytic degradation, a simplified pathway is proposed for the MIL-53(Fe)/H_2O_2 system under visible light. Upon irradiation, MIL-53(Fe) absorbs visible photons, promoting electrons from the Valence Band (VB) to the Conduction Band (CB), resulting in the generation of electron–hole (e^-/h^+) pairs:

$$\text{MIL-53(Fe)} + hv \rightarrow h^+ + e^-$$

The photogenerated electrons can react with H_2O_2 to produce highly reactive hydroxyl radicals (•OH):

$$e^- + H_2O_2 \rightarrow \bullet OH + OH^-$$

Simultaneously, the holes (h^+) in the valence band can also oxidize H_2O or OH^- to form •OH radicals:

$$h^+ + H_2O \rightarrow \bullet OH + H^+$$

or

$$h^+ + OH^- \rightarrow \bullet OH$$

These hydroxyl radicals, along with other Reactive Oxygen Species (ROS) such as superoxide anions ($O_2\bullet^-$) formed through electron interaction with dissolved O_2, attack the chromophoric structure of Methyl Orange (MO), leading to its stepwise oxidative degradation:

$$\bullet OH \,/\, O_2\bullet^- + MO \rightarrow \text{intermediates} \rightarrow CO_2 + H_2O$$

This series of reactions ultimately results in the breakdown of MO into harmless end products. The role of MIL-53(Fe) is not only to harvest visible light but also to facilitate redox cycling through its Fe(III)/Fe(II) centers, enhancing ROS generation and electron–hole separation. The presence of H_2O_2 acts as both an electron acceptor and a source of •OH, significantly improving degradation efficiency. This mechanism is consistent with general AOP pathways and supported by previous studies on iron-based photocatalysts [28, 39]. The combined use of MIL-53(Fe) and H_2O_2 significantly accelerates the degradation rate compared to photocatalysis or Fenton-like reactions alone [37]. Moreover, the MOF's porosity facilitates dye adsorption and proximity to reactive sites, further supporting effective degradation [40].

Overall, the proposed mechanism supports the experimental observations of high degradation efficiency and offers insight into the role of ROS and catalyst structure in promoting sustainable dye treatment under solar or visible-light conditions.

The synthesis method developed in this study is a novel, modified solvothermal approach for producing MIL-53(Fe). This technique offers significant advantages over conventional methods by drastically reducing both the reaction time and energy input. Unlike typical procedures that require 12–24 h, this method achieves successful crystallization in just 2 h at a moderate temperature of 150 °C. Furthermore, post-synthesis purification is simplified to a cost-effective and environmentally friendly process involving only an overnight soak in distilled water, eliminating the need for solvent-intensive purification techniques. This streamlined method yields MIL-53(Fe) with exceptional performance, exhibiting a 98.75% degradation efficiency of MO under visible light without the need for additional dopants or sensitizers. The practical benefits and high efficiency of this synthesis underscore its strong potential for use in real-world wastewater treatment applications.

While this study successfully demonstrates the synthesis and effective photocatalytic performance of MIL-53(Fe) for methyl orange degradation, several key limitations warrant consideration for future research. A comprehensive cost analysis related to the synthesis process was not included, which limits the assessment of economic feasibility for large-scale implementation. Additionally, key factors such as water stability and mechanical stability were not investigated, both of which are crucial for evaluating the long-term structural integrity under operational conditions. Reusability and operational stability were also not examined through repeated degradation cycles or post-reaction characterization. Addressing these limitations will facilitate a more comprehensive evaluation of MIL-53(Fe) for sustainable applications in wastewater treatment systems.

V. Conclusion

This study demonstrates the promising potential of MIL-53(Fe), an iron-based metal–organic framework, as a visible-light-responsive photocatalyst for the degradation of MO in simulated textile wastewater. Comprehensive material characterization and controlled degradation experiments showed that the MIL-53(Fe)/H_2O_2/visible light system achieved a remarkable maximum dye removal efficiency of 98.75% under optimal conditions, with reaction kinetics following a pseudo-first-order model. The system maintained robust performance across a wide pH range, with pH 3 identified as the optimal condition. Importantly, balancing H_2O_2 dosage and reaction time was critical to maximizing hydroxyl radical generation while minimizing scavenging effects.

Control trials confirmed the synergistic interaction among the catalyst, oxidant, and light, driving a Fenton-like mechanism, where hydroxyl radicals (•OH) and photogenerated holes (h^+) are the primary reactive species responsible for dye degradation. These findings establish MIL-53(Fe) as a highly efficient, stable, and operationally tunable photocatalyst compatible with solar-simulated light, making it a compelling candidate for sustainable wastewater treatment solutions. The demonstrated high degradation efficiency, combined with operational flexibility and environmental compatibility, underscores the system's potential for real-world application in textile wastewater treatment. The synergistic effect among photocatalyst, H_2O_2, and visible light is critical in optimizing degradation performance, highlighting the importance of precise control over reaction parameters.

Future research should focus on a comprehensive evaluation of the long-term reusability and regeneration of the MIL-53(Fe) photocatalyst. To bridge the gap between laboratory findings and practical applications, it is essential to scale up the synthesis process for industrial use and rigorously assess its performance in treating complex, real-world wastewater effluents. Further investigations should also be directed toward optimizing reactor design, establishing the long-term mechanical and chemical stability of the catalyst, and broadening its applicability to a broader range of organic pollutants. These efforts will be crucial for

fully realizing the potential of MIL-53(Fe) in advancing sustainable and effective wastewater treatment technologies.

Conflict of Interest

The authors declare no conflict of interest.

Author Contributions

Chloe Justin Bigornia, Yna Isabel Dimaano, and Quinn Lendyll Teope conducted the research; Eden S. Erasga, Chloe Justin Bigornia, Yna Isabel Dimaano, and Quinn Lendyll Teope analyzed the data; Eden S. Erasga, Chloe Justin Bigornia, Yna Isabel Dimaano, and Quinn Lendyll Teope wrote the full paper; all authors had approved the final version.

Acknowledgment

The authors wish to thank Mapua Institute of Technology at Laguna, Mapua Malayan Colleges Laguna, Chemistry Laboratory, and IFO-CHM Office.

References

[1] D. A. Yaseen and M. Scholz, "Textile dye wastewater characteristics and constituents of synthetic effluents: A critical review," *International Journal of Environmental Science and Technology*, vol. 16, no. 2, pp. 1193–1226, 2019.

[2] E. S. Erasga, A. R. Matienzo, A. J. N. Nanola, and A. J. B. Vibar, "Adsorption of methylene blue dye from aqueous solution using activated cogon grass (Imperata cylindrica) fixed on alginate," *Chemical Engineering Transactions*, vol. 113, pp. 265–270, 2024.

[3] A. Mishra, R. S. Singh, V. Mishra, B. S. Giri, and D. Singh, "Kinetics studies and effect of the process parameters on the biodegradation of methyl orange dye," *Journal of the Indian Chemical Society*, vol. 101, no. 10, 101334, 2024.

[4] A. Zuorro and R. Lavecchia, "Evaluation of UV/H_2O_2 Advanced Oxidation Process (AOP) for the degradation of diazo dye Reactive Green 19 in aqueous solution," *Desalination and Water Treatment*, vol. 52, no. 7–9, pp. 1571–1577, 2014.

[5] E. Oyarce, B. Butler, P. Santader, and J. Sanchez, "Polyelectrolytes applied to remove methylene blue and methyl orange dyes from water via polymer-enhanced ultrafiltration," *Journal of Environmental Chemical Engineering*, vol. 9, no. 6, 106297, 2021.

[6] F. Raji, M. Zafari, A. Rahbar-Kelishami, and S. G. Ashrafizadeh, "Enhanced removal of methyl orange using modified anion exchange membrane adsorbent," *International Journal of Environmental Science and Technology*, vol. 20, no. 9, pp. 9823–9836, 2023.

[7] X. Shao, J. Wang, Z. Liu, N. Hu, M. Liu, C. Duan, R. Zhang, and C. Quan, "Cellulose based cation-exchange fiber as filtration material for the rapid removal of methylene blue from wastewater," *Cellulose*, vol. 28, no. 14, pp. 9355–9367, 2021.

[8] H. O. Jamel, M. H. Jasim, M. A. Mahdi, S. H. Batool, L. S. Jasim, and M. N. Haider, "Adsorption of Rhodamine B dye from solution using 3-((1-(4-((1H-benzo [d] imidazol-2-yl) amino) phenyl) ethylidene) amino) phenol (BIAPEHB)/P (AA-co-AM) composite," *Desalination and Water Treatment*, vol. 321, 101019, 2025.

[9] A. S. Umesh, Y. M. Puttaiahgowda, and S. Thottathil, "Enhanced adsorption: Reviewing the potential of reinforcing polymers and hydrogels with nanomaterials for methylene blue dye removal," *Surfaces and Interfaces*, vol. 51, 104670, 2024.

[10] W. Qin, Y. Dong, H. Jiang, W. H. Loh, J. Imbrogno, T. M. Swenson, O. Garcia-Rodriguez, and O. Lefebvre, "A new approach of simultaneous adsorption and regeneration of activated carbon to address the bottlenecks of pharmaceutical wastewater treatment," *Water Research*, vol. 252, 121180, 2024.

[11] H. B. Rahmoun, M. Boumediene, A. N. Ghenim, E. F. da Silva, and J. Labrincha, "Coupling coagulation–flocculation–sedimentation with adsorption on biosorbent (corncob) for the removal of textile dyes from aqueous solutions," *Environments*, vol. 12, no. 6, 201, 2025.

[12] S. Sonal and B. K. Mishra, "Role of coagulation/flocculation technology for the treatment of dye wastewater: Trend and future aspects," *Water Pollution and Management Practices*, Singapore: Springer Singapore, pp. 303–331, 2021.

[13] M. S. Lucas, A. R. Teixeira, N. Jorge, and J. A. Peres, "Industrial wastewater treatment by coagulation–flocculation and advanced oxidation processes: A review," *Water*, vol. 17, no. 13, 1934, 2025.

[14] J. L. Wang and L. J. Xu, "Advanced oxidation processes for wastewater treatment: Formation of hydroxyl radical and application," *Critical Reviews in Environmental Science and Technology*, vol. 42, no. 3, pp. 251–325, 2012.

[15] C. Lopez-Lopez, J. Martín-Pascual, M. V. Martínez-Toledo, M. M. Muñío, E. Hontoria, and J. M. Poyatos, "Kinetic modelling of TOC removal by H_2O_2/UV, photo-Fenton and heterogeneous photocatalysis processes to treat dye-containing wastewater," *International Journal of Environmental Science and Technology*, vol. 12, no. 10, pp. 3255–3262, 2015.

[16] D. H. da Silva Santos, Y. Xiao, N. Chaukura, J. M. Hill, R. Selvasembian, C. L. S. Zanta, and L. Meili, "Regeneration of dye-saturated activated carbon through advanced oxidative processes: A review," *Heliyon*, vol. 8, no. 8, e10205, 2022.

[17] S. Foteinis, A. G. Borthwick, Z. Frontistis, D. Mantzavinos, and E. Chatzisymeon, "Environmental sustainability of light-driven processes for wastewater treatment applications," *Journal of Cleaner Production*, vol. 182, pp. 8–15, 2018.

[18] B. Hayati, N. M. Mahmoodi, M. Oveisi, A. Panahdar, M. Bakhtiari, S. Langari, K. Seifpanahi-Shabani, and H. Marzban, "Synthesis of iron based-metal-organic framework nanocomposite and visible light pollutant degradation ability," *Materials Research Bulletin*, vol. 138, 111243, 2021.

[19] M. Pu, Z. Guan, Y. Ma, J. Wan, Y. Wang, M. L. Brusseau, and H. Chi, "Synthesis of iron-based metal-organic framework MIL-53 as an efficient catalyst to activate persulfate for the degradation of Orange G in aqueous solution," *Applied Catalysis A: General*, vol. 549, pp. 82–92, 2018.

[20] H. Liu, W. W. Yi, Q. Q. Li, and S. Y. Zhao, "Visible-light-active benzothiadiazole-based MOFs as efficient ROS generators for the synthesis of benzimidazoles and benzothiazoles," *Inorganic Chemistry Frontiers*, vol. 11, no. 18, pp. 5973–5978, 2024.

[21] S. B. Bagherzadeh, M. Kazemeini, and N. M. Mahmoodi, "A study of the DR23 dye photocatalytic degradation utilizing a magnetic hybrid nanocomposite of MIL-53(Fe)/$CoFe_2O_4$: Facile synthesis and kinetic investigations," *Journal of Molecular Liquids*, vol. 301, 112427, 2020.

[22] W. S. Koe, J. W. Lee, W. C. Chong, Y. L. Pang, and L. C. Sim, "An overview of photocatalytic degradation: Photocatalysts, mechanisms, and development of photocatalytic membrane," *Environmental Science and Pollution Research*, vol. 27, no. 3, pp. 2522–2565, 2020.

[23] J. J. Du, Y. P. Yuan, J. X. Sun, F. M. Peng, X. Jiang, L. G. Qiu, A. J. Xie, Y. H. Shen, and J. F. Zhu, "New photocatalysts based on MIL-53 metal–organic frameworks for the decolorization of methylene blue dye," *Journal of Hazardous Materials*, vol. 190, no. 1–3, pp. 945–951, 2011.

[24] M. S. Samuel, K. V. Savunthari, and S. Ethiraj, "Synthesis of a copper (II) metal–organic framework for photocatalytic degradation of rhodamine B dye in water," *Environmental Science and Pollution Research*, vol. 28, no. 30, pp. 40835–40843, 2021.

[25] A. S. Munn, A. J. Ramirez-Cuesta, F. Millange, and R. I. Walton, "Interaction of methanol with the flexible metal-organic framework MIL-53(Fe) observed by inelastic neutron scattering," *Chemical Physics*, vol. 427, pp. 30–37, 2013.

[26] J. López, A. M. Chávez, A. Rey, and P. M. Álvarez, "Insights into the stability and activity of MIL-53(Fe) in solar photocatalytic oxidation processes in water," *Catalysts*, vol. 11, no. 4, 448, 2021.

[27] P. Dinh Du, H. Thanh Danh, P. Ngoc Hoai, N. M. Thanh, V. Thang Nguyen, and D. Quang Khieu, "Heterogeneous UV/Fenton-like degradation of methyl orange using iron terephthalate MIL-53 catalyst," *Journal of Chemistry*, vol. 2020, pp. 1–13, 2020.

[28] L. Ai, C. Zhang, L. Li, and J. Jiang, "Iron terephthalate metal–organic framework: Revealing the effective activation of hydrogen peroxide for the degradation of organic dye under visible light irradiation," *Applied Catalysis B: Environmental*, vol. 148, pp. 191–200, 2014.

[29] T. Loiseau, C. Serre, C. Huguenard, G. Fink, F. Taulelle, M. Henry, T. Bataille, and G. Férey, "A rationale for the large breathing of the porous aluminum terephthalate (MIL-53) upon hydration," *Chemistry–A European Journal*, vol. 10, no. 6, pp. 1373–1382, 2004.

[30] D. T. C. Nguyen, H. T. N. Le, T. S. Do, V. T. Pham, D. Lam Tran, V. T. T. Ho, T. V. Tran, D. C. Nguyen, L. G. Bach, H. K. P. Ha, and V. T. Doan, "Metal-organic framework MIL-53(Fe) as an adsorbent for ibuprofen drug removal from aqueous solutions: Response surface modeling and optimization," *Journal of Chemistry*, vol. 2019, 5602957, 2019.

[31] S. Yu, H. Zhang, and C. Li, "Solvothermal in-situ synthesis of MIL-53 (Fe)@ carbon felt photocatalytic membrane for rhodamine B

degradation," *International Journal of Environmental Research and Public Health*, vol. 20, no. 5, 4571, 2023.
[32] F. A. Sofi and K. Majid, "Enhancement of the photocatalytic performance and thermal stability of an iron based metal–organic-framework functionalised by Ag/Ag_3PO_4," *Materials Chemistry Frontiers*, vol. 2, no. 5, pp. 942–951, 2018.
[33] N. Stock and S. Biswas, "Synthesis of metal-organic frameworks (MOFs): Routes to various MOF topologies, morphologies, and composites," *Chemical Reviews*, vol. 112, no. 2, pp. 933–969, 2012.
[34] J. López, A. M. Chávez, A. Rey, and P. M. Álvarez, "Insights into the stability and activity of MIL-53 (Fe) in solar photocatalytic oxidation processes in water," *Catalysts*, vol. 11, no. 4, 448, 2021.
[35] G. Chaturvedi, A. Kaur, and S. K. Kansal, "CdS-decorated MIL-53 (Fe) microrods with enhanced visible light photocatalytic performance for the degradation of ketorolac tromethamine and mechanism insight," *The Journal of Physical Chemistry C*, vol. 123, no. 27, pp. 16857–16867, 2019.
[36] A. Karami, A. R. Shomal, R. Sabouni, M. H. Al-Sayah, and A. Aidan, "Parametric study of methyl orange removal using metal–organic frameworks based on factorial experimental design analysis," *Energies*, vol. 15, no. 13, 4642, 2022.
[37] Y. Zhang, S. Zhang, H. Guo, B. Liu, H. Zhang, J. Xiao, R. Yang, Y. Yin, and X. Pei, "Rapid degradation of high-concentration antibiotic via heterogeneous photocatalysis coupling Fenton-like oxidation with MIL-53(Fe) under visible light irradiation," *Colloids and Surfaces A: Physicochemical and Engineering Aspects*, vol. 694, 134114, 2024.
[38] Y. Qu, Z. Chen, Y. Duan, and L. Liu, "H2O2 assisted photocatalysis over Fe-MOF modified BiOBr for degradation of RhB," *Journal of Chemical Technology & Biotechnology*, vol. 97, no. 10, pp. 2881–2888, 2022.
[39] X. Hu and B. Jin, "The performance and mechanism of a MIL-53 (Fe)/$ZnIn_2S_4$ heterophase photo-Fenton system in degrading p-nitrophenol," *New Journal of Chemistry*, vol. 49, no. 9, pp. 3545–3556, 2025.
[40] X. Chen, X. Liu, L. Zhu, X. Tao, and X. Wang, "One-step fabrication of novel MIL-53 (Fe, Al) for synergistic adsorption-photocatalytic degradation of tetracycline," *Chemosphere*, vol. 291, 133032, 2022.

Copyright © 2026 by the authors. This is an open access article distributed under the Creative Commons Attribution License which permits unrestricted use, distribution, and reproduction in any medium, provided the original work is properly cited (CC BY 4.0).